RSC Advances

ROYAL SOCIETY OF CHEMISTRY

www.rsc.org/advances

Dissociation of O_2 and Its Reactivity on O/S doped Graphene

MeilingHou[1], WanglaiCen[2,3]*, Fang Nan[4], JianjunLi[1,3], Yinghao Chu[1,3*], HuaqiangYin[1,3]

1. College of Architecture and Environment, Sichuan University, Chengdu, 610065, P. R. China;

2. Institute of New Energy and Low Carbon Technology, Sichuan University, Chengdu, 610065, P. R. China;

3. National Engineering Research Center for Flue Gas Desulfurization, Chengdu, 610065, P. R. China;

4. Sichuan Electric Design and Consulting Company, Chengdu, 610094, P. R. China.

Corresponding Authors:

Dr. Wanglai Cen (cenwanglai@163.com)

Dr. Yinghao Chu(chuyinghao@scu.edu.cn)

Tel/Fax: +86 28 85401682

Abstract

It was routinely believed that the oxidation of SO_2 to SO_3 dominates the removal rate of SO_2 on carbon-based catalysts. Recently, both experiments and theoretical calculations evidence that SO_2 is readily oxidized by epoxy groups on graphene oxides at room temperature. Based on this point, we hypothesized in this work that the real rate-determining step for SO_2 catalytic oxidation under O_2 atmosphere could be the dissociation of molecular O_2, which further forms oxygen funtional groups on graphene surface. Density functional theory corrected with dispersion was employed to investigate the dissociation of O_2 on O or S doped graphene and then their reactivity for SO_2 oxidation. This results showed that O/S doping greatly promotes the dissociation, leading to the formation of epoxy and/or carbonyl groups on the graphene surface. However, the high oxidation barrier for the oxidation of SO_2 by carbonyl group was found, which implicates carbonyl group is of low reactivity. Therefore, dopants screening or doped structures design should be carefully considered to avoid the formation of carbonyl during O_2 dissociation.

Keywords: First principles, heteroatom doped graphene, desulfurization, oxygen functional group

1 Introduction

Sulfur dioxide (SO_2) is one of the notorious pollutants with toxicity released by the burning of fossil fuels, such as in automobile engines and power plants, which contributes greatly to acid deposition. A lot of efforts have been made to develop techniques for its treatment. Among them, carbon materials, typically activated carbon (AC) and activated carbon fibres (ACF), has long been known to be a general media for the catalytic removal of SO_2 at low temperature (20~150℃)[1-4]. But the mechanism at atomic level remains unclear, which hinders the development of more effective carbon-based catalysts for desulfurization.

It is conventionally thought that the rate-determining step for the catalytic removal of SO_2 by carbon is the oxidation of SO_2 into SO_3[5]. However, it was found that the oxidation could be catalyzed by graphene oxides (GO) at room temperature[6]. Addtionally, by density functional theory calculations, Zhang and coworkers[7,8] found that SO_2 can be oxidized by epoxy groups of GO with rather low energy barrier. Both experiemental and theoretical results indicate that epoxy groups should be the active center for the oxidation of SO_2, which might not be the rate-determing step. Alternatively, we hypothesized that the real rate-determining step in the oxidation of SO_2 might be the formation of epoxy groups from the dissociation of sluggish O_2.

Graphene (GP) can be used as a model catalyst to provide insights for the catalytic oxidation of SO_2 on carbon materials[6,9-11]. Doping with foreign atoms has been confirmed to be an effective functionalization method[12-16]. For example, N-doped graphene was found to be active for oxygen reduction reaction (ORR)[17-19]. The ORR is a four-electron pathway, which is believed to depend on the spin density and the atomic charge redistribution on the neighboring carbon atoms close to the doping sites.[18,20] Besides, Dai[21] et al. proposed that the high activity of N-doped GP may be

attributed to the larger electronegativity of N, which creates positive charge on the adjacent C atoms. These results indicate that other electonegative heteroatom doping and charge redistribution caused by them may favor the adsorption and reduction of O_2 as well. However, some low electronegative elements doping, such as boron[15,22], sulfur[23,24], or their mixture[25,26], have also promoted the catalytic activity of GP pronouncedly. Charged sites created by breaking the electroneutrality of GP might be the key factor, regardless of the electronegativity of doping atoms.[22]

In this work, S and O atoms were introduced into GP respectively, to investigate the probable dependence of O_2 molecule adsorption and dissociation on electronegativity of doping atoms, by using density functional theory (DFT) calculations. The electronegativity of S atom is 2.58, which is close to C atom. While the electronegativity of O is 3.44. It is much stronger than that of C atom. Both experimental[27] and theoretical results[27,28] indicate that the substitution of internal atoms in graphene by heteroatoms is the key role for the promoted catalytic activity of graphene materials. Therefore, only the substitution of internal C atom(s) by O/S atom will be considered. To determine the activity of oxygenic functional groups on the doped-graphene, the adsorption and oxidation of SO_2 on the doped materials has been calculated.

2 Models and methods

2.1 Computational models

$3\sqrt{3}\times6$ graphene unit cell (with 72 carbon atoms, GP) was employed as the model substrate as depicted in Figure 1a.It was large enough for the reaction $SO_2+1/2O_2\rightarrow SO_3$ according to our previouswork[7,8]. A vacuum region of 20 Å was added perpendicular to the graphene plane to minimize the interaction between different layers[29]. Single O atom took the place of one C atoms

(Figure 1b), denoted as OG. Single S atom took the place of two neighboring C atoms (Figure 1c), denoted as SG. The relaxed bond lengths of C-C in GP are 1.42 Å, which are consistent with experimental data. The relaxed C-O bonds and C-S bonds are 1.48 and 1.86 Å, respectively. Although it has been confirmed that S can been doped in the plane of GP, the local structures remains unclear[23]. We have tested two doping models: with single S atom replacing one and two internal C atom(s). It was found the latter is more feasible (Figure S1-S3). Therefore, only the two C atoms replaced model was used, and denoted as SG by default.

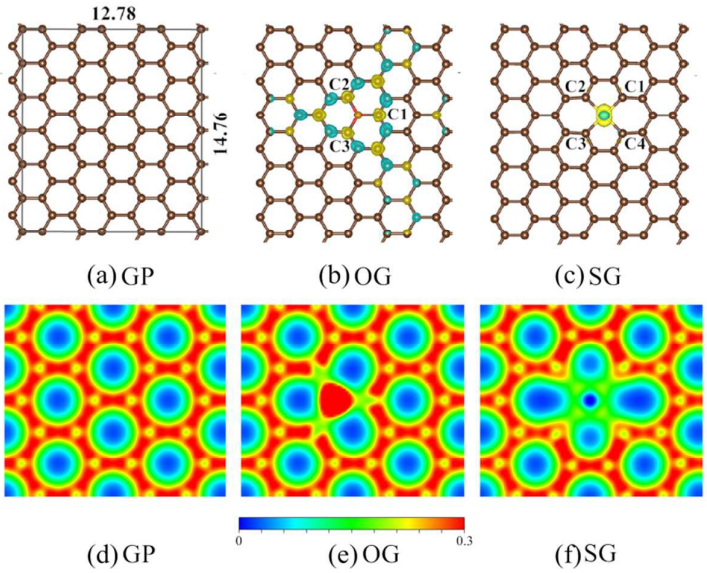

Figure 1 Spin density (a-c) and total charge density (d-f) analysis of different surfaces. GP, OG and SG stand for pristine, O doped and S doped graphene, respectively. All lengths are given in Å. The isosurface for (a)-(c) is 5E-6 e/Å^3.

2.2 Computational methods

All the density functional theory (DFT) calculations were carried out with the code VASP5.2[30,31] using the generalized gradient approximation with a Perdew-Burke-Ernzerhof (PBE) exchange and correlation functional[32]. A plane-wave basis set with cut-off energy 400 eV was employed within the framework of the projector augmented-wave (PAW) method[33].The Brillouin zone was sampled

with a 3×3×1 k-points sampled with Monkhorst-Pack method. Gaussian smearing was used, with a smearing width 0.2 eV. The D2 method of Grimme[34] was used to describe the van der Waals (vdW) correction with default parameters. All the atoms except those on the boundary were relaxed and converged to 0.02 eV/Å. The carbon atoms on the boundary of the GP substrate were frozen in all directions. All the above parameters were sufficient to ensure the total energy converge to within 1 meV/atom. The calculated bond lengths of C-C in graphene and O-O in isolated O_2 molecule are 1.42 and 1.26 Å, respectively, which are consistent with published values[35,36]. Nudged elastic band (NEB) method[37,38] was used to search the minimum reaction pathway (MEP) of O_2 reduction by heteroatom-doped graphene from an initial state (IS) to its final state (FS) with 8-12 replicas interpolated. Transition state (TS) was localized with climbing image method and verified with single imaginary frequency.

The adsorption energy ΔE_{ads} is defined as

$$\Delta E_{\text{ads}} = E_{\text{tot}} - (E_{\text{mol}} + E_{\text{sheet}})$$

Where E_{tot}, E_{mol}, and E_{sheet} are the total energies of the adsorption complex, the isolated molecule and the GP/doped-GP sheet, respectively.

3 Results

3.1 S and O doped Graphene

We first focus on the electronic structures of pristine and doped-graphene. It was believed that spin density and positive charge can be introduced by electronegative atoms doping, which was of importance for catalytic activity promotion. The spin density determines the positional selectivity of radical adsorption, while charge density determines the adsorption energy[20]. Figure 1b shows that spin density was induced by O doping, in a pattern up and down alternately among 1~4 C

atoms from the dopant. While the spin was localized at the S atom for SG as demonstrated in Figure 1c. Charge density in Figure 1e illustrates electrons were transferred from C1~C3 atoms to the dopant O atom, which results in positive charged C atoms for species adsorption. The redistribution of charge densities of C atoms in SG is almost unperceivable. Consequently, the order for the catalytic activity of the three different samples might be GP < SG < OG and the C atoms directly connected to dopants should be regarded as active sites. Density of states (DOS) analysis showed that the main electron structures S and O doped GP were remained as that of pristine GP (Figure S4).

3.2 Adsorption and dissociation of O_2 molecule

3.2.1 O_2 adsorption

The adsorptions of O_2 on GP，OG and SG surfaces have been calculated both with non- and spin polarization, as shown in Figure 2a-c and Figure 2d-f, respectively. Spin polarization seems to relieve the adsorption of O_2 by pristine or doped planes, as the distances from the adsorbed O_2 to the substrates are much longer by 0.1~0.3 Å than that without spin polarization. In both conditions, O_2 is pull closer to the surface in case of S/O doping. For the adsorption of O_2 on GP, the adsorbed O_2 is parallel above GP surface, with a distance 3.13 Å (Figure 2d), which is in good agreement with published value of 3.09 Å[39]. The adsorption distances are increased in the order OG < SG < GP. However, all the bond lengths of adsorbed O_2 are *ca.* 1.26 Å (Table 1), quite close to the value of isolated gaseous molecule, denoting that only physisorption exists.

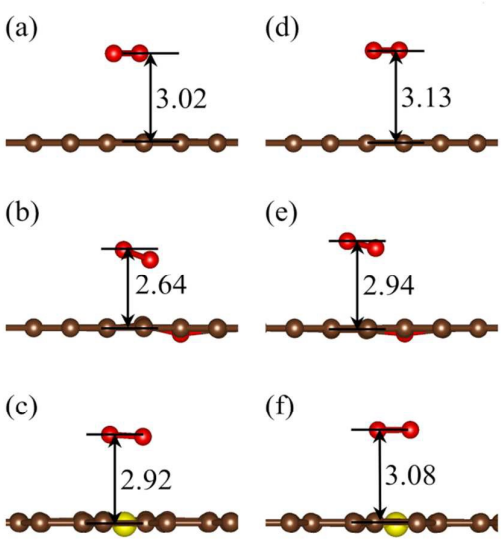

Figure 2 Relaxed adsorption configurations of O_2 on GP, OG and SG surfaces. Spin polarization was ignored in (a)-(c), while it was included for (d)-(f). All the distances are given in Å.

As tabulated in Table 1, the adsorption energies obtained with spin polarization are lower than those with non-spin polarization correspondingly, and the adsorption energies increase in the order GP < SG < OG, both of which are consistent with the geometric trends mentioned above. The adsorption energy of O_2 on GP in Figure 2d is 0.14 eV. It is also in good agreement with previous calculated value of 0.11 eV[39], while a little larger than the experimentally tested value of 0.1 eV[40].

Based on geometric and energetic results, spin polarization possesses few effects and can be ignored for qualitative conclusions.

Table 1 Summary of adsorption energy for the adsorption O_2 on GP, OG and SG surface.

Conf.	O_2/GP		O_2/SG		O_2/OG	
	NSP[a]	SP[b]	NSP	SP	NSP	SP
ΔE_{ads}, eV	0.34	0.13	0.36	0.16	0.57	0.26
O-O bond length, Å	1.26	1.25	1.27	1.25	1.26	1.26

a: Non-spin polarization; b: Spin polarization.

3.2.2 O_2 dissociation

Figure 3 shows the MEP for oxygen dissociation reaction on pristine GP. Totally, the oxygen dissociation on GP is endothermic by 0.72 eV, indicating that the process is thermodynamically unfavorable. During the dissociation process, a middle state (MS) emerged, which divided the reaction into two sections. In the MS configuration, the two oxygen atoms and the two carbon atoms right under them formed a square, with side length of 1.50 Å. From IS to MS, the energy barrier is 1.78 eV, and a net energy consumption by 1.23 eV. During the process, O_2 is pulled closer to the carbon basal plane. The bond length of the O-O bond in the initial state (IS) is 1.26 Å, which is equal to the calculated bond length of isolated O_2 molecule in gaseous phase. The TS1 is more similar to the middle state (MS) than the reactant (IS) in geometric structure. The controlling factor seems to be pulling the O_2 molecule close to the substrate and elongate the O-O bond to form peroxide ion O_2^{2-}. From MS to FS, the energy barrier is 0.62 eV, with a net energy release by 0.51 eV. In the final state (FS), the bond lengths of the O-C bonds are 1.45 or 1.48Å, which are equivalent to the bond length of epoxy. Finally, O_2 molecule was dissociated and transferred to two epoxy groups endothermically with rather high a barrier, implying the reaction on pristine graphene is unfeasible under mild conditions.

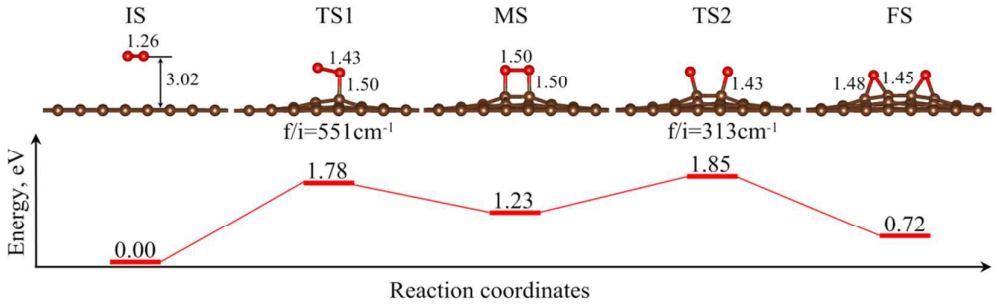

Figure 3 Minimum energy pathway (MEP) for the dissociation of oxygen on pristine graphene (GP). All the lengths are given in Å.

The MEP for the oxygen dissociation on doped-GP was demonstrated as Figure 4 for OG and Figure 5 for SG. On the approaching of O_2 to OG (from IS to MS), the bond length of O_2 was elongated from 1.26 to 1.38 Å, where O_2 was converted to O_2^- (superoxide ion). The barrier of this process was about 0.01 eV according to our testing calculations, with a net energy release by 2.04 eV. The C atom connected to the adsorbed O_2 was drawn out of the OG surface, which was one of the nearest C atoms originally connected to the doped O atom.

From MS to FS in Figure 4, the reaction energy barrier is as low as 0.05 eV, with a net energy release by 1.07 eV. During this process, the O_2^- was pulled closer to the substrate. The bond length of the O-O bond was further elongated from 1.38 Å to 1.41 Å in TS, and then2.68 Å in FS, which means the O-O bond in oxygen was broken thoroughly. The determining step seems to be the breaking of the O-O bond of the adsorbed superoxide ion. After the dissociation, one O atom of O_2 molecule was connected with two C atoms on the OG surface to form epoxy group, and the other with one C atom to form carbonyl group. The two bonds of the epoxy are about 1.48 and 1.42 Å, which are in accordance with the calculation results in Ref.8.

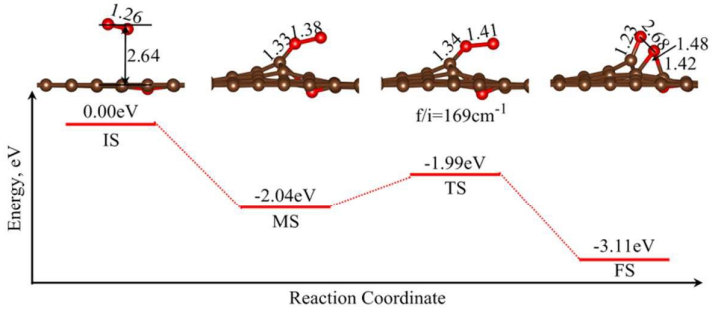

Figure 4 Minimum energy pathway (MEP) for the dissociation of oxygen on O-doped graphene (OG). All the lengths are giver in Å.

The MEP of O_2 dissociation on SG was shown in Figure 5. There are also two energy barriers for the dissociation of O_2, and obviously the first energy barrier is the main one, with a value of

0.39 eV. Similar to the situation on GP, the determining step was the activation of adsorbed O_2 molecule to form superoxide ion, with O-O bond elongated from 1.26 to 1.34 Å. Then the O-O bond was further elongated, with a barrier 0.19 eV to form two carbonyl groups (FS), with the O-C bond length 1.23 Å.

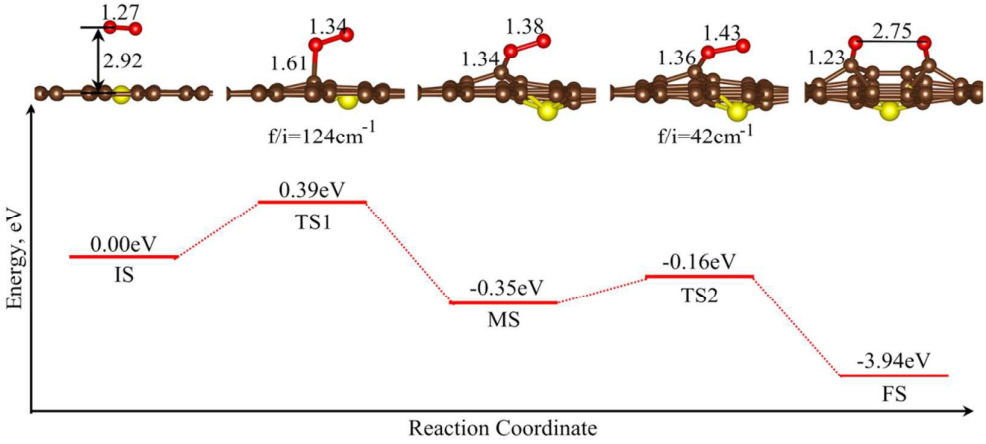

Figure 5 Minimum energy pathway (MEP) for the dissociation of oxygen on S-doped graphene (SG). All the lengths are given in Å.

3.3 SO_2 oxidation by dissociated O_2

It has been known that heteroatom doping can promote the dissociation of oxygen on graphene. However, the reactivity of the formed oxygen groups are unknown. Hence, we test the oxidation of SO_2 on two doped-GPs. For conciseness, we denoted the dissociated adsorption configuration of O_2 on OG(SG) as 2O_OG (2O_SG). When one oxygen group was consumed through oxidation reaction, the left species was denoted as 1O_OG (1O_SG). Selected adsorption and reaction energies for SO_2 oxidation were listed in Table 2. Combined with energetic data analysis for the dissociation of O_2, it is interesting to found that both the two catalytic loops are thermodynamically favorable. However, the rate-determining step for the catalytic oxidation of SO_2 by OG is SO_2/1O_OG→SO_3/OG, with a barrier of 2.46 eV, and that by SG for SO_2/2O_SG→

199 SO_3/1O_SG is 2.57 eV. Both of the two pathways are not kinetically promising as expected as
200 their rate-determining barriers are unsatisfactory.

201 Table 2 Summary of adsorption energies (ΔE_{ads}), energy barriers (E_b) and reaction energies (E_r)
202 for the adsorption of SO_2/SO_3 on different surfaces

Adsorption	ΔE_{ads}, eV	Reaction	E_b, eV	E_r, eV
SO_2/2O_OG	−0.35	SO_2/2O_OG→SO_3/1O_OG	0.79	-1.79
SO_2/1O_OG	−0.46	SO_2/1O_OG→SO_3/OG	2.46	1.48
SO_2/2O_SG	−0.27	SO_2/2O_SG→SO_3/1O_SG	2.57	0.62
SO_2/1O_SG	−0.37	SO_2/1O_SG→SO_3/SG	1.41	-0.03

203 According to previous researches[6,8], epoxy group should be responsible for the high activity of
204 graphene oxides for the oxidation of SO_2. When O_2 was dissociated on OG, a epoxy group and a
205 carbonyl group were formed in configuration 2O_OG. While for 2O_SG, there were two carbonyl
206 groups formed. Carbonyl group was supposed to be sluggish for oxidation. The MEP for the
207 oxidation of SO_2 by 2O_OG was shown in Figure 6 to provide some clues for further
208 understanding of the oxidation mechanism.

209 During the first section from IS to MS, the epoxy group was transferred to carbonyl group as
210 well, with a small barrier 0.23 eV. The oxidation barrier from MS to FS was 0.79 eV, with a net
211 energy release by 1.79 eV. Such high a barrier confirms that carbonyl group is inertial for
212 oxidation. It is quite different for the oxidation of SO_2 by epoxy group located on pristine GP[8],
213 where the barrier is as low as *ca.* 0.2 eV. The main difference should be the extension of O-C bond
214 during oxidation. For epoxy group, the O-C bond was extended from 1.48 to 1.81Å, with a
215 extension 0.33 Å. While for carbonyl group, the O-C bond was extended from 1.27 to 1.62 Å, with

a extension 0.35 Å. The shorter initial O-C bond length and the longer extension results in much higher oxidation barrier. Accordingly, it is rationally expected that the barriers for oxidation processes SO_2/1O_OG→SO_3/OG, SO_2/2O_SG→SO_3/1O_SG and SO_2/1O_SG→SO_3/SG are also much higher, as carbonyl groups were involved.

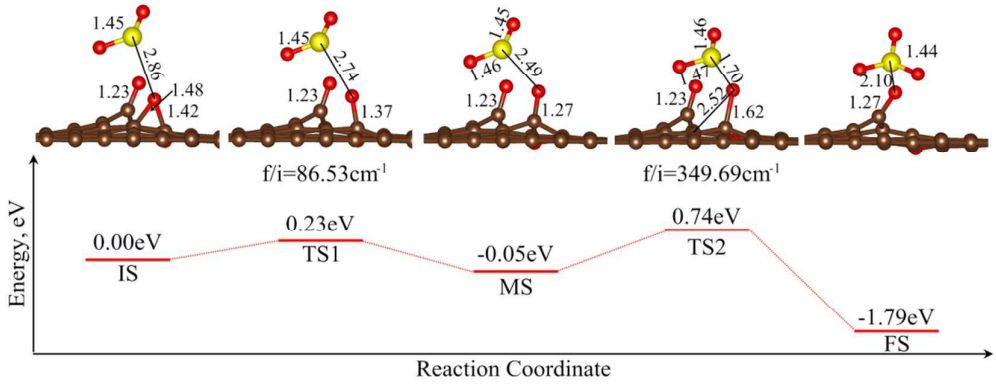

Figure 6 Minimum energy pathway (MEP) for the oxidation of SO_2 by 2O_OG. All the lengths are given in Å.

4. Discussion

It has been found that the dissociation of O_2 on graphene can be well promoted by heteroatoms doping, but the oxidation activities of oxygen species derived from O_2 dissociation are quite different and still unsatisfactory. Herein, attention will be paid to the electronic structures of different oxygen species to get a fundamental understanding.

As shown in Figure 7, compared with the situation of the epoxy group on GP (Figure 7a), the valence band of the epoxy group on OG (Figure 7b) is shifted to lower level. Besides the shift of the primary highest occupied molecular orbital (HOMO, marked as A in the plot), a new peak (marked as B) presents in Figure 7b. It implies that the epoxy group of OG is more inertial than that of GP. Figure 7c shows a low level peak (marked as C) present below -20 eV. It confirms that carbonyl group is quite sluggish for oxidation, as it is prohibitive cost of energy to activate it.

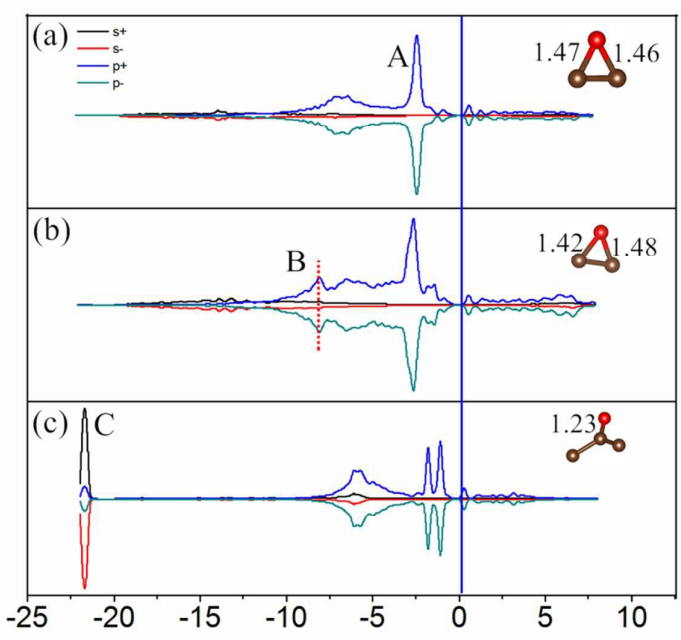

Figure 7 Density of states (DOS) analysis for oxygen functional groups on different surfaces. (a) epoxy group on GP surfaces, (b) epoxy group on OG surfaces, (c) carbonyl group on SG surface.

Based on electronic structure analysis, it was found that the formation of highly active epoxy group from O_2 dissociation should be the key point for design and synthesis of graphene-based catalysts for redox. In the present study, both the O and S doping resulted in the formation of carbonyl group, which is inertial in catalytic oxidation process. Other dopants or doping patterns might be more promising.

5 Conclusion

Density functional theory corrected with dispersion was used to investigate the potential promotion effects of O and S doping in graphene on oxygen dissociation and catalytic oxidation of SO_2. It was found that O/S doping tremendously promotes the dissociation of sluggish molecular oxygen, which leads epoxy and/or carbonyl groups formed on the doped graphene surfaces. Due to the formation of carbonyl group, the catalytic loop for the oxidation of SO_2 was terminated for its high oxidation barrier. These results indicated that more attentions should be paid on dopants

249 screening or doped structures design to avoid the formation of carbonyl in O_2 dissociation. Further
250 exploration is needed to screen other dopants or doping patterns.

251 **Acknowledgements**

252 This work was financially supported by the National Natural Science Foundation of China
253 (51508356, 51378325) and Young Talent Program for Science and Technology Innovation of
254 Sichuan Province in China (2015040). We also acknowledge the National Supercomputer Center
255 in Shenzhen of China for computational service support.

256 **References:**

257 (1)X. Liu, J. Guo, Y. Chu, D. Luo, H. Yin, M. Sun, and R. Yavuz, Desulfurization performance of
258 iron supported on activated carbon, *Fuel*, 2014, **123**, 93-100.
259 (2)Y. Qu, J. Guo, Y. Chu, M. Sun, and H. Yin, The influence of Mn species on the SO_2 removal of
260 Mn-based activated carbon catalysts, *Appl. Sur. Sci.*, 2013. **282**,. 425-431.
261 (3)D. L. ´pez, R. Buitrago, A. S. ´lveda-Escribano, F. R. ´guez-Reinoso, and F. M. ´n, Low
262 temperature catalytic adsorption of SO_2 on activated carbon, *J. Phys. Chem. C.*, 2008. **112**,
263 15335-15340.
264 (4)N. Karatepe, R. Y. İlkün Orbakb, and A. Özyuğuranb, Sulfur dioxide adsorption by activated
265 carbons having different textural and chemical properties, *Fuel*, 2008. **87**, 3207-3215.
266 (5)A. A. Lizzio, J. A. DeBarr, Mechanism of SO_2 removal by carbon, *Energ. Fuels*, 1997.
267 **11**,284-291.
268 (6)Y. Long, C. Zhang, X. Wang, J. Gao, W. Wang, and Y. Liu, Oxidation of SO_2 to SO_3 catalyzed
269 by graphene oxide foams, *J. Mater. Chem.*, 2011. **21**, 13934.
270 (7)H. Zhang, W. Cen, J. Liu, J. Guo, H. Yin, and P. Ning, Adsorption and oxidation of SO_2 by
271 graphene oxides: A van der Waals density functional theory study, *Appl. Sur. Sci.*, 2015. **324**,
272 61-67.
273 (8)W. Cen, M. Hou, J. Liu, S. Yuan, Y. Liu, and Y. Chu, Oxidation of SO_2 and NO by epoxy
274 groups on graphene oxides: the role of the hydroxyl group, *RSC Adv.*, 2015. **5**, 22802-22810.
275 (9)C. Huang, C. Li, and G. Shi, Graphene based catalysts, *Energ. Environ. Sci.*, 2012. **5**,

8848-8868.

(10)S. Tang and Z. Cao, Adsorption of nitrogen oxides on graphene and graphene oxides: Insights from density functional calculations, *J. Phy. Chem. Phy.*, 2011. **134**,. 044710-1~044710-14.

(11)M. Hou, W. Cen, H. Zhang, J. Liu, H. Yin, and F. Wei, Adsorption and oxidation of NO on graphene oxides: A dispersion corrected density functional theory investigation, *Appl. Sur. Sci.*, 2015. **339**, 55-61.

(12)Z. Mo, R. Zheng, H. Peng, H. Liang, and S. Liao, Nitrogen-doped graphene prepared by a transfer doping approach for the oxygen reduction reaction application, *J. Power Sources*, 2014. **245**, 801-807.

(13)J. Bai, Q. Zhu, Z.Lv, H. Dong, J. Yu, and L. Dong, Nitrogen-doped graphene as catalysts and catalyst supports for oxygen reduction in both acidic and alkaline solutions, *Int. J. Hydrogen Energ.*, 2013. **38**, 1413-1418.

(14)Z. Ma, S. Dou, A.Shen, L. Tao, L.Dai, and S. Wang, Sulfur-dopend graphene derived from cycled lithium-sulfur batteries as a metal-free electrocatalyst for the oxygen reduction reaction, *Ang. Chem. Int. Ed.*, 2015. **54**, 1888-1892.

(15)S. Wang, L. Zhang, Z. Xia, A. Roy, D. Chang, J. B. Baek, and L. Dai, BCN Graphene as efficient metal-free electrocatalyst for the oxygen reduction reaction, *Ang. Chem. Int. Ed.*, 2012. **51**, 4209-4212.

(16)M. Li, L. Zhang, Q. Xu, J.Niu, and Z. Xia, N-doped graphene as catalysts for oxygen reduction and oxygen evolution reactions: Theoretical considerations, *J. Catal.*, 2014. **314**, 66-72.

(17)C. H. Choi, M. W. Chung, H. C. Kwon, J. H. Chung, and S. I. Woo, Nitrogen-doped graphene/carbon nanotube self-assembly for efficient oxygen reduction reaction in acid media, *Appl. Catal. B: Environ.*, 2014. **144**, 760-766.

(18)L. Zhang and Z. Xia, Mechanisms of oxygen reduction reaction on nitrogen-hoped graphene for fuel cells, *J. Phys. Chem. C.*, 2011. **115**, 11170-11176.

(19)Q. Liu, H. Zhang, H. Zhong, S. Zhang, and S. Chen, N-doped graphene/carbon composite as non-precious metal electrocatalyst for oxygen reduction reaction, *Electrochim. Acta.*, 2012. **81**, 313-320.

(20)L. Zhang, J. Niu, L. Dai, and Z. Xia, Effect of microstructure of nitrogen-doped graphene on

oxygen reduction activity in fuel cells, *Langmuir*, 2012. **28**, 7542–7550.

(21)K. Gong, F. Du, Z. Xia, M. Durstock, L. Dai, Nitrogen-doped carbon nanotube arrays with high electrocatalytic activity for oxygen. *Science*, 2009, **323**, 760-763.

(22)L. Yang, S. Jiang, Y. Yu, L. Zhu, S. Chen, X. Wang, Q. Wu, J. Ma, Y. Ma, and Z. Hu., Boron-doped carbon nanotubes as metal-free electrocatalysts for the oxygen reduction reaction, *Ang. Chem. Int. Ed.*, 2011. **50**, 7132-7135.

(23)Z. Yang, Z. Yao, G. Li, G. Fang, H. Nie, L. Zheng, X. Zhou, X. Chen, and S. Huang, Sulfur-doped graphene as an efficient metal-free cathode catalyst for oxygen reduction, *ACS Nano*, 2012. **6**, 205-211.

(24)I. Y. Jeon, S. Zhang, L. Zhang, H. J. Choi, J. M. Seo, Z. Xia, L. Dai, and J. B. Baek, Edge-selectively sulfurized graphene nanoplatelets as efficient metal-free electrocatalysts for oxygen oeduction oeaction: The electron spin effect, *Adv. Mater.*, 2013. **25**, 6138-6145.

(25)J. Liang, Y. Jiao, M. Jaroniec, and S. Qiao, Sulfur and nitrogen dual-doped mesoporous graphene electrocatalyst for oxygen reduction with synergistically enhanced performance, *Ang. Chem. Int. Ed.*, 2012. **51**, 11496-11500.

(26)Y. Zheng, Y. Jiao, L. Ge, M. Jaroniec, and S. Qiao, Two-step boron and nitrogen doping in graphene for an enhanced synergistic catalysis, *Ang. Chem. Int. Ed.*, 2013. **52**, 3110-3116.

(27)Gao, Y.; Hu, G.; Zhong, J.; Shi, Z.; Zhu, Y.; Su, D. S.; Wang, J.; Bao, X.; Ma, D., Nitrogen-doped sp^2-hybridized carbon as a superior catalyst for selective oxidation, *Ang. Chem. Int. Ed.*, 2013, **52**, 2109-2113.

(28)Boukhvalov, D. W.; Son, Y. W.; Ruoff, R. S., Water splitting over graphene-based catalysts: Ab initio calculations, *ACS Catal.*, 2014, **4**, 2016-2021.

(29)M. Yang, M. Zhou, A. Zhang, C. Zhang, Graphene oxide: An ideal support for gold nanocatalysts, *J. Phys. Chem. C.*, 2012, **116**, 22336-22340.

(30)G. Kresse, J. Furthmuller, Efficiency of ab-initio total energy calculations for metals and semiconductors using a plane-wave basis set, *Comp. Mater. Sci.* 1996, **6**, 15-50.

(31) G. Kresse, J. Furthmuller, Efficient iterative schemes for ab initio total-energy calculations using a plane-wave basis set, *Phys. Rev. B.* 1996, **54**, 11169-11186.

(32)J. P. Perdew, K. Burke, M. Ernzerhof, Generalized gradient approximation made simple, *Phys. Rev. Lett.* 1996, **77**, 3865-3868.

(33)G. Kresse, D. Joubert, From ultrasoft pseudopotentials to the projector augmented-wave method, *Phys. Rev. B.* 1999, **59**, 1758-1775.

(34)S. Grimme, Semiempirical GGA-type density functional constructed with a long-range dispersion correction, *J. Comput. Chem.* 2006, **27**, 1787-1799.

(35)D. R. Lide, Handbook of chemistry and physics, 84th edition, *CRC Press*, **2003**.

(36)E. Fuente, J. A. Menendez, M. A. Diez, D. Suarez, M. A. Montes-Moran, Infrared spectroscopy of carbon materials: A quantum chemical study of model compounds, *J. Phys. Chem. B.* 2003, **107**, 6350-6359.

(37)G. Henkelman, H. Jonsson, Improved tangent estimate in the nudged elastic band method for finding minimum energy paths and saddle points, *J. Chem. Phys.* 2000, **113**, 9978-9985.

(38)G. Henkelman, B. P. Uberuaga, H. Jonsson, A climbing image nudged elastic band method for finding saddle points and minimum energy paths, *J. Chem. Phys.*2000, **113**, 9901-9904.

(39)A. Pramanik, H. S. Kang, Density functional theory study of O_2 and NO adsorption on heteroatom-doped graphene including the van der Waals interaction, *J. Phys. Chem. C.*2011, **115**, 10971-10978.

(40)G. Vidali, G. Ihm, Potentials of physical adsorption, *Surf. Sci. Rep.* 1991, **12**, 133-181.

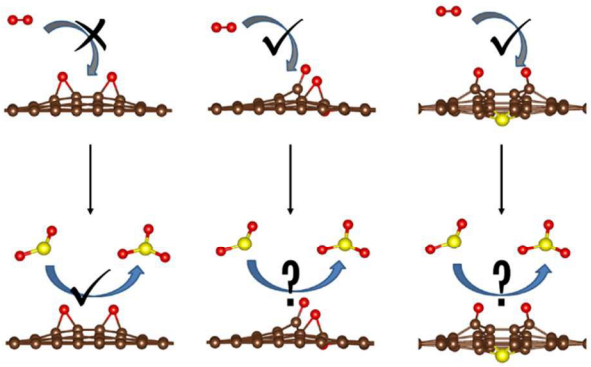

O/S doping tremendously promotes the dissociation of sluggish molecular oxygen, which leads epoxy and/or carbonyl groups formed on the doped graphene surfaces. While, the catalytic loop for the oxidation of SO_2 was terminated for its high oxidation barrier due to the formation of carbonyl group.